Difluoroboron Dibenzoylmethane PCL-PLA Block Copolymers: Matrix Effects on Room Temperature Phosphorescence

Guoqing Zhang, Gina L. Fiore, Tyler L. St. Clair, and Cassandra L. Fraser*

Department of Chemistry, University of Virginia, McCormick Road, P.O. Box 400319, Charlottesville, Virginia 22904

Received January 12, 2009; Revised Manuscript Received February 24, 2009

ABSTRACT: Luminescent materials result when boron dyes are combined with polyester biomaterials. Previously, it was reported that difluoroboron dibenzoylmethane polylactide, BF_2dbmPLA, exhibits intense fluorescence as well as unusual room temperature phosphorescence (RTP) in the solid state. To gain a better understanding of polymer effects on photophysical properties, a poly(ε-caprolactone) (PCL) analogue, BF_2dbmPCL, was synthesized by tin catalyzed ring-opening polymerization and employed as a macroinitiator in combination with D,L- and L-lactide for the preparation of BF_2dbmPCL-PLA and BF_2dbmPCL-PLLA block copolymers, respectively. Reasonably well-defined materials with low polydispersity indices (PDIs) were obtained in good yield. ^{1}H NMR and UV−vis spectroscopy and thermal analysis are reported. Luminescence spectra and lifetimes were measured for polymer solutions and films. All materials are intensely fluorescent with high quantum yields. Although no RTP is noted for BF_2dbmPCL films, curiously, this property is restored for PCL-polylactide block copolymer analogues in the solid state.

Introduction

The incorporation of boron dyes into polymers results in optical materials with impressive, tunable properties.[1−4] For example, luminescent difluoroboron dibenzoylmethane-polylactide (BF_2dbmPLA), composed of a BF_2dbm[5] headgroup and a covalently attached poly(lactic acid) (PLA) tail, shows intense fluorescence and unusual room-temperature phosphorescence (RTP) in the solid state.[6] The fluorescence of BF_2dbmPLA can be conveniently tailored by its molecular weight (MW), exhibiting green-to-blue emission depending on the length of the PLA chain.[7] This approach to fluorescence color tuning involves alterations in dye interactions via changes in the surrounding medium.[8] The large Stokes shift and long lifetime of RTP can eliminate interference from autofluorescence and excitation scattering in luminescence spectroscopic analysis.[9] Furthermore, the high sensitivity of RTP to the environment (e.g., matrix[10] and quenchers[11]) can be used to monitor protein dynamics,[12] electron[13] and energy[14] transfer, temperature variations,[15] and oxygen level changes.[16] As a readily processable polymeric material, BF_2dbmPLA can be fabricated as films, fibers, and water-stable nanoparticles[17] that retain solid-state optical features, including RTP, in aqueous media, making it a promising candidate for imaging, sensing, and many other applications.

Thus far, our investigations have largely focused on PLA as a dye matrix because it figures prominently in green chemistry[18] and sustainable[19] design as the demand for new kinds of biorenewable polymeric materials is on the rise while crude oil reserves are decreasing. Apart from its role as a plastic in sustainable packaging,[20] as a biodegradable and biocompatible polymer, PLA also finds wide use in biomedical fields such as drug delivery and tissue engineering.[21] Another type of polyester, poly(ε-caprolactone) (PCL), is also extensively utilized as a biomaterial.[22] Although PCL and PLA are similar polyesters, compositional differences make PCL a more flexible, hydrophobic, and crystalline polymer that is slower to degrade than PLA.[23] Given the prevalence of PCL in tissue engineering matrices and long circulating drug delivery vehicles,[24] and the desire to understand matrix composition and physical property effects on boron dye optical properties, we explored the synthesis and optical properties of BF_2dbmPCL.[25] Curiously, no RTP is observed for this material, which we hypothesize may be attributed to differences in polymer states (i.e., glassy vs rubbery or crystalline, viscosity, rigidity) compared with PLA at a given temperature. With controlled polymerization, BF_2dbmPCL may also be used as a macroinitiator for the synthesis of BF_2dbmPCL-PLA and BF_2dbmPCL-PLLA block copolymers with different degrees of polymerization for further fine-tuning of materials properties, for example, in thermoplastics[26] or drug delivery systems.[27] PLA stereochemistry (D,L- vs L-, referred to here as PLA and PLLA, respectively) has been reported to affect material performance and degradation,[28,29] and it could also influence boron dye optical properties. In addition, we investigate whether PCL-PLA block copolymers exhibit optical properties that are characteristic of PCL, PLA, or some composite of these two components. Thermal and photophysical properties of boron polymers are also reported. The introduction of a light-emitting dye adds imaging and sensing capability to PCL-PLA hybrid materials, which can be useful for many applications.

Experimental Section

Materials. The boron initiator, BF_2dbmOH, was prepared as previously reported.[6] ε-Caprolactone was dried over CaH_2 and distilled under reduced pressure prior to use. 3,6-Dimethyl-1,4-dioxane-2,5-dione (D,L-lactide, Aldrich) and (3*S*)-*cis*-3,6-dimethyl-1,4-dioxane-2,5-dione (L-lactide, Aldrich) were recrystallized from ethyl acetate (2×) and stored in a drybox under a nitrogen atmosphere. Tin(II) 2-ethylhexanoate ($Sn(oct)_2$, Spectrum) and all other reagents were used as received.

Methods. ^{1}H NMR (300 MHz) spectra were recorded on a Varian UnityInova spectrometer in $CDCl_3$ unless otherwise indicated. Resonances were referenced to the signal for residual protiochloroform at 7.260 ppm. ^{1}H NMR coupling constants are given in hertz. UV−vis spectra were recorded on a Hewlett-Packard 8452A diode-array spectrophotometer in CH_2Cl_2. Molecular weights were determined by gel permeation chromatography (GPC) (THF, 25 °C, 1.0 mL/min) using multiangle laser light scattering (MALLS) (λ = 633 nm, 25 °C) and refractive index (RI) (λ = 633 nm, 40 °C) detection. A Polymer Laboratories 5 μm mixed-C guard column and two GPC columns along with Wyatt Technology (Optilab DSP

* To whom correspondence should be addressed. E-mail: fraser@virginia.edu.

10.1021/ma9000622 CCC: $40.75
Published on Web 04/01/2009

Scheme 1

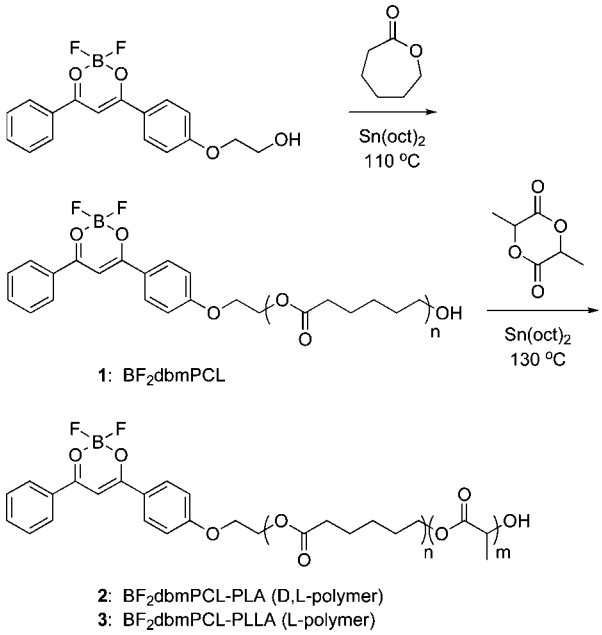

interferometric refractometer, DAWN DSP laser photometer) and Agilent Technologies instrumentation (series 1100 HPLC) and Wyatt Technology software (ASTRA) were used in GPC analysis. The incremental refractive indices (d*n*/dc values) for polymer samples were determined by a single injection method that assumed 100% mass recovery from the columns. Thermogravimetric analysis (TGA) was conducted using a TA Instruments TGA 2050 thermogravimetric analyzer from 30 to 500 °C with a heating/cooling rate of 10 °C/min under N_2. Differential scanning calorimetry (DSC) measurements were performed using a TA Instruments DSC 2920 modulated DSC. Analyses were carried out in modulated mode under a nitrogen atmosphere (amplitude = ±1 °C; period = 60 s; heating rate = 5 °C/min; range −10 to 200 °C). Reported values of thermal events are from the second heating cycle and the reversing heat flow curve unless otherwise indicated (T_d = onset point of decomposition; T_m reported as the peak maximum).

A Laurell Technologies WS-650S spin-coater was used to cast polymer films for luminescence measurements. Powders were analyzed as precipitated. Steady-state fluorescence emission spectra were recorded on a Horiba Fluorolog-3 model FL3-22 spectrofluorometer (double-grating excitation and double-grating emission monochromators). RTP spectra were recorded with the same instrument except that a pulsed xenon lamp (λ_{ex} = 396 nm; duration <1 ms) was used and spectra were collected with a 1 ms delay after excitation. Time-correlated single-photon counting (TCSPC) fluorescence lifetime measurements were performed with a NanoLED-370 (369 nm) excitation source and DataStation Hub as the SPC controller. Phosphorescence lifetimes were measured with a 500 ns multichannel scalar (MCS) excited with a pulsed xenon lamp (λ_{ex} = 396 nm; duration <1 ms). Lifetime data were analyzed with DataStation v2.4 software from Horiba Jobin Yvon.

BF_2dbmPCL$_2$, 1. This material was prepared as previously reported.[25] Synthesis and characterization data for the macroinitiator **1** are provided. A dry Kontes flask was charged with BF_2dbmOH (0.053 g, 0.159 mmol) and ε-caprolactone (2.74 g, 24.0 mmol) under a nitrogen atmosphere. The flask was sealed and placed in an oil bath at 110 °C to create a homogeneous melt. Under a flow of nitrogen, a stock solution of Sn(oct)$_2$ (1.62 mg, 4.00 μmol) in hexanes was added to the reaction mixture. The reaction vessel was resealed and heated at 110 °C until an extremely viscous mixture resulted (~24 h). The reaction mixture was cooled to room temperature, dissolved in a minimal amount of CH_2Cl_2, and precipitated by dropwise addition to cold stirring hexanes (−78 °C). The supernatant was decanted, and the solid residue was washed with cold hexanes and dried in vacuo to afford BF_2dbmPCL as a yellow solid: 1.87 g (68%). ^{1}H NMR (300 MHz, $CDCl_3$, δ): 8.16 (t, *J* = 9.0, 2′,6′-Ar*H*, 2″,6″ Ar*H*), 7.69 (t, *J* = 8.3, 4′-Ar*H*), 7.55 (m, 3″,5″ Ar*H*), 7.13 (s, COC*H*CO), 7.05 (d, *J* = 8.9, 3′,5′-Ar*H*), 4.48 (d, *J* = 4.5, CH_2CH_2OAr), 4.30 (m, CH_2CH_2OAr), 4.06 (t, *J* = 6.5, RCO_2CH_2), 2.30 (t, *J* = 7.5, CH_2CO_2R), 1.70−1.56 (m, CH_2), 1.43−1.32 (m, CH_2). M_w (MALLS) = 11 100, PDI = 1.07, d*n*/dc = 0.078 mL/g.

Table 1. Molecular Weight Data for Boron Polyesters

polymer	M_n (NMR)	M_n[c]	M_w[c]	PDI[c]	time (h)	yield (%)
BF_2dbmPCL	12 300[a]	10 400[d]	11 100[d]	1.07	24	68
BF_2dbmPCL-PLA	12 200[b]	11 200[e]	12 900[e]	1.15	2.5	53
	22 700[b]	18 600[f]	22 300[f]	1.20	5.5	43
BF_2dbmPCL-PLLA	13 000[b]	11 100[g]	13 200[g]	1.19	2.1	65
	16 500[b]	15 000[h]	19 300[h]	1.29	8	30

[a] Estimated from the relative integration of PCL $-RCO_2CH_2-$ (4.06 ppm) and dbm (8.16 ppm) peaks. [b] Determined from the relative integration of PCL $-RCO_2CH_2-$ (4.06 ppm) and PLA $-CH-$ (5.27 to 5.11 ppm) or PLLA $-CH-$ (5.16 ppm) peaks using GPC (MALLS) M_n for the first block. [c] Molecular weight data determined by GPC (MALLS) in THF. [d] Molecular weight data estimated using the d*n*/d*c* value for PCL (0.078 mL/g). [e] d*n*/dc = 0.070 mL/g. [f] d*n*/dc = 0.053 mL/g. [g] d*n*/dc = 0.069 mL/g. [h] d*n*/dc = 0.054 mL/g.

BF_2dbmPCL-PLA, 2. A representative procedure is provided. A dry Kontes flask was charged with BF_2dbmPCL (0.304 g, 0.029 mmol, 10 400 Da) and D,L-lactide (0.152 g, 1.05 mmol). The flask was evacuated, backfilled with nitrogen, sealed, and immersed in an oil bath at 130 °C to create a homogeneous melt. Under a flow of nitrogen, a 27.8 mM solution of Sn(oct)$_2$ in hexanes (21 μL, 0.5 μmol) was added to the reaction mixture. The reaction vessel was resealed and heated to 130 °C until an extremely viscous mixture resulted (2.5 h). The reaction mixture was cooled to room temperature, dissolved in a minimal amount of CH_2Cl_2, and precipitated by dropwise addition to cold stirring hexanes (−78 °C). The supernatant was decanted, and the solid residue was reprecipitated (2×) from CH_2Cl_2/hexanes (−78 °C) and washed with cold hexanes. The polymer was then reprecipitated from CH_2Cl_2/MeOH (−78 °C) and dried in vacuo to afford BF_2dbmPCL-PLA as an off-white solid: 0.242 g (53%, uncorrected for monomer conversion). ^{1}H NMR (300 MHz, $CDCl_3$, δ): 5.27−5.11 (m, C*H*), 4.06 (t, *J* = 6.7, RCO_2CH_2), 2.31 (t, *J* = 7.5, CH_2CO_2R), 1.70−1.52 (m, CH_2, CH_3), 1.43−1.33 (m, CH_2). M_w (MALLS) = 12 900, PDI = 1.15, d*n*/dc = 0.070 mL/g.

BF_2dbmPCL-PLLA, 3. The PLLA diblock samples were synthesized as described for **2**. The low molecular weight sample (Table 1) was prepared with the following loadings: BF_2dbmPCL (0.303 g, 0.029 mmol, 10 400 Da), L-lactide (0.162 g, 1.12 mmol), and a solution of Sn(oct)$_2$ in hexanes (21 μL, 27.8 mM, 0.5 μmol). BF_2dbmPCL-PLLA was obtained as a yellow solid: 0.303 g (65%, uncorrected for monomer conversion). ^{1}H NMR (300 MHz, $CDCl_3$, δ): 5.16 (q, *J* = 7.1, C*H*), 4.06 (t, *J* = 6.7, RCO_2CH_2), 2.31 (t, *J* = 7.5, CH_2CO_2R), 1.70−1.55 (m, CH_2, CH_3), 1.43−1.33 (m, CH_2). M_w (MALLS) = 13 200, PDI = 1.19, d*n*/dc = 0.069 mL/g.

Quantum Yield Measurements. Fluorescence quantum yields, Φ_F, for BF_2dbmPCL, BF_2dbmPCL-PLA, and BF_2dbmPCL-PLLA in CH_2Cl_2 were calculated versus anthracene in EtOH as a standard, as previously described[30] using the following values: Φ_F anthracene = 0.27,[31] n_D^{20} EtOH = 1.360, and n_D^{20} CH_2Cl_2 = 1.424. Optically dilute CH_2Cl_2 solutions of BF_2dbmPCL, BF_2dbmPCL-PLA, and BF_2dbmPCL-PLLA and EtOH solutions of the anthracene standard were prepared in 1 cm path length quartz cuvettes, and absorbances (A < 0.1) were recorded and steady-state emission spectra were obtained (λ_{ex} = 350 nm; emission integration range: 365−700 nm).

Film Preparation. Boron polymer films were spin-cast from CH_2Cl_2 solutions (~2.5% w/w) onto Fischer Scientific glass cover slides (22 × 22 mm) at the spin speed of 4000 rpm. The coated slides were cut into 3 × 22 mm^2 strips, placed in a transparent glass vial under a N_2 atmosphere, and sealed with Teflon caps for measurements. (Note: Both borosilicate glass cover slides and glass vials are optically inactive using excitation wavelength of >368 nm.)

Results and Discussion

Boron polyester materials, BF_2dbmPCL, BF_2dbmPCL-PLA, and BF_2dbmPCL-PLLA, were prepared via controlled ring-opening polymerization. The BF_2dbmPCL macroinitiator was prepared using hydroxyl-functionalized BF_2dbmOH (Scheme 1) as the initiator via $Sn(oct)_2$ catalyzed ring-opening polymerization (ROP) of ε-caprolactone at 110 °C.[25] After heating for 24 h and purification by precipitation from hexanes, BF_2dbmPCL (M_n = 10 400 Da, PDI = 1.07) was obtained in good yield (68%; uncorrected for monomer consumption). Growth of the polymer from the hydroxyl initiator site is further supported by ^{1}H NMR analysis, wherein the BF_2dbmCH_2CH_2OH initiator protons (4.23 and 4.04 ppm) have shifted to higher field (4.48 and 4.30 ppm) after polymerization. The signal attributable to the initiator hydroxyl group at 1.96 ppm disappears, and resonances corresponding to PCL in the 1.70 to 1.56 ppm range are evident. Subsequently, lactide was polymerized from the PCL hydroxyl chain end to form diblock copolymers. Two stereoisomers of lactide monomer, namely, D,L-lactide and L-lactide, were used to synthesize BF_2dbmPCL-PLA and BF_2dbmPCL-PLLA, respectively. The block polymerizations were run using BF_2-dbmPCL as the macroinitiator for $Sn(oct)_2$ catalyzed, solvent-free lactide polymerization at 130 °C. For each stereodiblock copolymer, two different PLA chain lengths were prepared using the same BF_2dbmPCL macroinitiator as the starting material. Reaction times range from 2−8 h depending on the lactide monomer and block length.

Molecular weight data for the BF_2dbm-containing polymers are provided in Table 1, and representative GPC traces are shown in Figure 1. GPC traces are fairly symmetrical, and PDIs remain low (≤1.2), although low MW shoulders were observed for certain polymer samples, suggesting incomplete macroinitiation and mixtures of block copolymer and macroinitiator in some cases, which is not uncommon, particularly for solvent-free reactions. The 3-D correlation of the GPC elution volume and inline diode array UV−vis spectra (Figure 2) for a BF_2dbmPCL-PLA sample confirms boron dye association with the eluting block copolymer.

The boron polymers were also analyzed by ^{1}H NMR spectroscopy in $CDCl_3$ solution. The molecular weight of BF_2dbmPCL was estimated by relative integration of BF_2dbm aromatic resonances versus polymer peaks (Table 1); however, end group signals were not evident in ^{1}H NMR spectra for block copolymer samples. This is typical for higher-molecular-weight polyester materials.[32] The ^{1}H NMR spectra for BF_2dbmPCL-PLA and BF_2dbmPCL-PLLA are shown in Figure 3. Characteristic PCL and PLA signals are observed (PCL: −RCO_2CH_2−, 4.06 ppm; −RCH_2CO_2−, 2.31 ppm; and −CH_2−, 1.70−1.52 and 1.43−1.33 ppm. PLA: −CH−, 5.27−5.11 ppm; −CH_3, 1.57 ppm. PLLA: −CH−, 5.16 ppm; −CH_3, 1.58 ppm). The spectra for PLA- and PLLA-containing samples are nearly identical except that the −CH− signal from 5.27−5.11 ppm is a multiplet for the D,L-polymer, whereas the L-polymer resonance at 5.16 ppm is a quartet. Molecular weights for diblocks were determined by ^{1}H NMR spectroscopy via relative integration of PCL and PLA peaks, using GPC (MALLS) M_n values for the first block. These values show good correspondence with GPC (MALLS) molecular weights measured for the diblock samples.

Thermal analysis data for the boron PCL macroinitiator and PCL-PLA and PCL-PLLA block copolymers are provided in Table 2. The BF_2dbmPCL decomposition temperature, 355 °C, is typical for PCL homopolymers, indicating that the dye has little effect on polymer thermal decomposition. In block copolymers the decomposition temperatures range from 349−380 °C.[33] Decomposition temperatures corresponding to PLA and PLLA segments are typically ∼262 °C, which is lower than the T_d for pure PLA, as reported.[34] Endothermic melting processes for PCL and PCL-PLA materials show characteristic temperatures for semicrystalline PCL ($T_m \approx$ 52−55 °C).[35] Crystallization temperatures for PCL segments are comparable in the homopolymer and the PCL-PLLA block copolymer (33, 37 °C) but depressed when interspersed with amorphous PLA (22, 26 °C). In PCL-PLLA block copolymers, both segments are semicrystalline, and melting events corresponding to each block are observed. Recently, Lemmouchi et al.[35] prepared PCL-PLLA materials with L-lactide monomer loadings of ∼25% and higher, and associated T_m values for the PLLA domains are typically ∼155 °C.[35] Here, too, PCL-PLLA block copolymers show a melting endotherm at 150 °C for the block copolymer with a longer PLLA segment, but in the case of a very short PLLA segment, a lower T_m value was observed (131 °C), suggesting a less-ordered material. Similarly, crystallization of the two blocks is also noted upon cooling. Materials with a

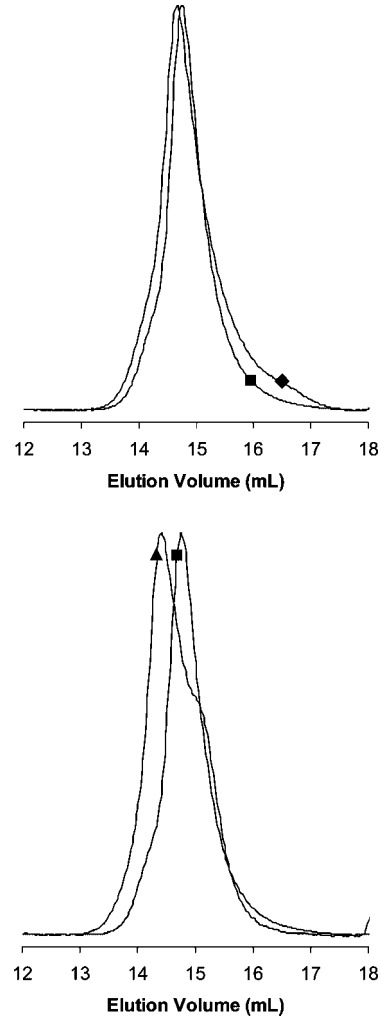

Figure 1. GPC overlay of the BF_2dbmPCL macroinitiator, M_n = 10 400, PDI = 1.07 (■) and two BF_2dbmPCL-PLA samples with different PLA degrees of polymerization (M_n = 11 200, PDI = 1.15 (◆) and M_n = 18 600, PDI = 1.20 (▲)).

Table 2. Thermal Analysis Data for Boron Dye−Polymer Conjugates

polymer	M_n (kDa)	T_c (°C)	T_m (°C)	$T_{d\ PLA}$ (°C)[a]	$T_{d\ PCL}$ (°C)[a]
BF_2dbmPCL	10.4	33	55		355
BF_2dbmPCL-PLA	11.2	26	52/55	262	349
	18.6	22	53	270	380
BF_2dbmPCL-PLLA	11.1	37/95	55/131	258	349
	15.0	33/115	54/150	262	366

[a] Determined from the onset temperature for decomposition for the indicated block.

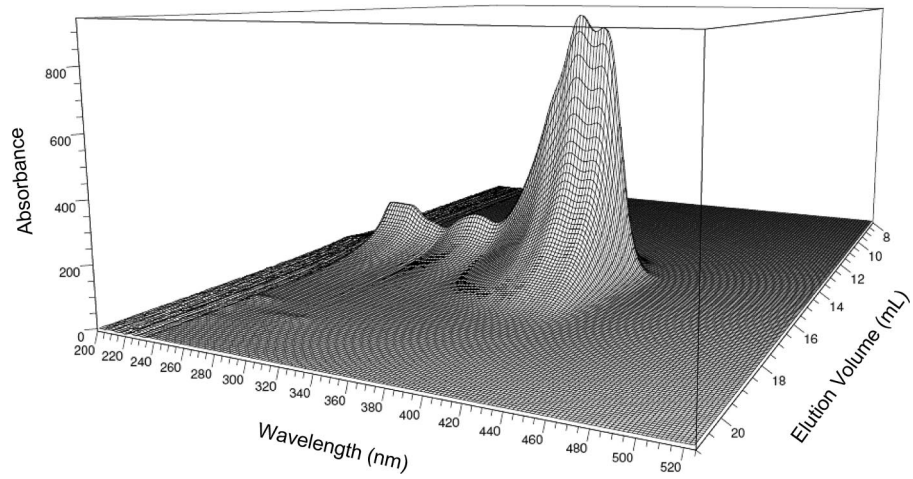

Figure 2. 3-D plot of GPC elution volume versus inline diode array UV−vis spectra for BF_2dbmPCL-PLA (M_n = 11 200, PDI = 1.15), showing that the BF_2dbm dye is associated with the eluting polymer fraction.

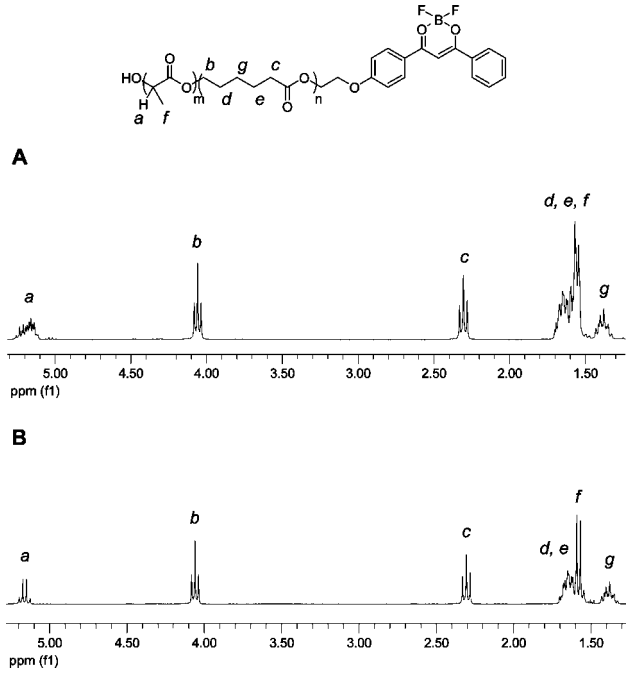

Figure 3. ^{1}H NMR spectra of (A) BF_2dbmPCL-PLA and (B) BF_2dbmPCL-PLLA in $CDCl_3$.

Table 3. UV-vis Absorption and Fluorescence Emission Data for Boron Polymers in CH_2Cl_2 Solution[a]

polymer	M_n (kDa)	ε (M^{-1} cm^{-1})	λ_{em} (nm)	τ (ns)	Φ_F
BF_2dbmPCL	10.4	34 500	430	1.91	0.72
BF_2dbmPCL-PLA	11.2	29 100	431	1.95	0.70
	18.6	32 200	430	1.97	0.81
BF_2dbmPCL-PLLA	11.1	31 400	430	1.96	0.78
	15.0	29 700	431	1.97	0.82

[a] λ_{ex} = 370 nm.

higher weight fraction of PLLA showed higher T_c value (115 vs 95 °C for the low molecular weight material).

The optical properties of boron-containing polymers were investigated for methylene chloride solutions, powders, and solid films. Solution data are provided in Table 3, and representative absorption and emission spectra are shown in Figure 4. All boron polymers, irrespective of the molecular weight and chemical compositions, exhibit almost identical emission properties in solution. Compared with previously reported values for BF_2dbmPLA in CH_2Cl_2 (e.g., M_n = 8800, λ_{em} = 396 nm, ε = 36 000 $M^{-1}cm^{-1}$, Φ_F = 0.89),[6] both boron PCL[25] and diblock copolymers have slightly lower extinction coefficients and comparable fluorescence quantum yields, Φ_F. These differences could be due to a polymer composition effect or possibly to the longer reaction times required for BF_2dbmPCL and diblock copolymer synthesis, which could result in a slight increase in degradation of the dye. The polymer composition and MW independent optical properties indicate that in solution the fluorophore mainly interacts with solvent molecules, and polymer chain effects are negligible. Delayed emission phenomena (i.e., phosphorescence or delayed fluorescence) are not observed for solutions at room temperature.

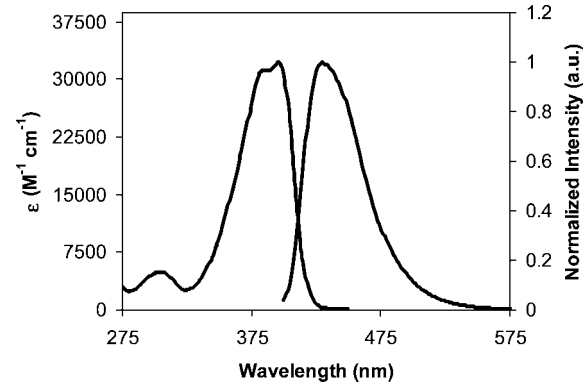

Figure 4. Representative absorption (λ_{max} = 396 nm) and emission (λ_{em} = 430 nm) spectra for a boron polymer, BF_2dbmPCL-PLA (M_n = 18 600), in CH_2Cl_2 solution.

The luminescence of boron polymers was also investigated in the solid state, for "as precipitated" powders and uniform films spin-cast on glass cover slides. Data for the powders and films are provided in Tables 4 and 5, respectively. Emission spectra are shown in Figures 5 and 6. As reported,[25] BF_2dbmPCL exhibits intense solid-state green-blue fluorescence (λ_{em} = 443 nm); however, the spectrum is broadened compared with spectral data for a BF_2dbmPLA film (M_n = 9500, λ_{em} = 440 nm).[7] Unlike BF_2dbmPLA, which shows strong and long-lived room temperature phosphorescence (λ_{em} = 509 nm, τ_{pw0} = 0.170 s)[6] under a nitrogen atmosphere (i.e., no O_2 quenching), no delayed emission was observed for BF_2dbmPCL films. The absence of RTP for oxygen-free, solid-state BF_2dbmPCL signals an important polymer composition effect on optical properties. The fluorescence emission of the BF_2dbmPCL macroinitiator was examined for powder and spin cast film forms. As seen in Figure 5, the film emission is more blue-shifted and exhibits a

Table 4. Luminescence Data for Boron Polymers as Powders

		fluorescence[a]				RTP[b]			
polymer	M_n (kDa)	λ_{em} (nm)	τ_F (ns)[c]	%[d]	τ_{pw0} (ns)[e]	λ_{em} (nm)	τ_{RTP} (ms)[f]	%[d]	τ_{pw0} (ms)[e]
BF_2dbmPCL	10.4	459	0.90	14	15.6				
			6.27	36					
			26.4	50					
BF_2dbmPCL-PLA	11.2	449	1.01	46	3.61	508	24.0	26	92.4
			2.93	37			76.8	60	
			12.1	17			286	14	
	18.6	446	1.33	51	3.54	518	50.7	18	266
			3.36	35			158	55	
			12.1	14			632	27	
BF_2dbmPCL-PLLA	11.1	450	0.96	42	4.07	522	21.6	17	106
			3.12	38			80.0	63	
			12.4	20			261	20	
	15.0	446	0.89	29	3.80	527	37.3	25	150
			2.65	48			119	59	
			9.90	23			458	16	

[a] λ_{ex} = 369 nm. [b] λ_{ex} = 396 nm. [c] Fluorescence lifetime. [d] Percentages represent pre-exponential weighted values. [e] Pre-exponential weighted lifetimes.[36] [f] Room temperature phosphorescence lifetime.

Table 5. Luminescence Data for Spin-Cast Boron Polymer Films

		fluorescence[a]				RTP[b]			
polymer	M_n (kDa)	λ_{em} (nm)	τ_F (ns)[c]	%[d]	τ_{pw0} (ns)[e]	λ_{em} (nm)	τ_{RTP} (ms)[f]	%[d]	τ_{pw0} (ms)[e]
BF_2dbmPCL	10.4	443	1.04	62	2.64				
			2.97	29					
			11.65	11					
BF_2dbmPCL-PLA	11.2	440	1.04	68	2.33	508	0.41	10	33.9
			2.82	24			6.34	32	
			11.59	8			54.99	58	
	18.6	429	0.97	57	2.18	518	2.75	6	154
			2.42	36			47.60	39	
			10.44	7			244.6	55	
BF_2dbmPCL-PLLA	11.1	442	0.51	44	2.61	523	0.22	25	22.1
			1.96	42			3.38	25	
			11.33	14			40.76	50	
	15.0	436	0.59	44	2.20	526	1.12	11	65.1
			1.82	46			14.24	31	
			9.53	10			105.8	58	

[a] λ_{ex} = 369 nm. [b] λ_{ex} = 396 nm. [c] Fluorescence lifetime. [d] Percentages represent pre-exponential weighted values. [e] Pre-exponential weighted lifetimes.[36] [f] Room temperature phosphorescence lifetime.

less broad low energy shoulder compared with its powder counterpart. Polymer processing has been previously described,[7] where fluorophore orientation and dye/substrate interaction could be involved.

For PCL-PLA diblock samples, the fluorescence emission maxima shift very slightly to higher energy (~440 nm, Tables 4 and 5 and Figure 5) compared with the BF_2dbmPCL homopolymer for both powders and films. Previously, it has been reported that fluorescence emission spectra are more sensitive to polymer MWs and processing conditions when the polymer MWs are below 10 kDa.[7,25] This could be due to a nonlinear relationship of fluorophore−fluorophore (F−F) interactions and the mean relative distance between them. Blue-shifted fluorescence for higher MW polymers in the solid-state has been ascribed to a reduction in F−F interactions in the excited state.[7] Despite the resemblance among the four fluorescence emission spectra, subtle differences are still perceivable. First, the spectra are slightly narrower for longer PLA chains. Polymers with higher MWs tend to show less of a vibronic tail in the lower energy region. Second, for diblock polymers, the L-stereoisomer shows broader and slightly red-shifted emission compared with its D,L-counterpart at comparable MWs. The observations were true for both powder and film samples, except that films exhibit broader spectral distribution. Yet, the most surprising result is that even a short PLA segment "turns on" the long-lived green RTP. Although the diblock copolymer RTP intensities are weaker than that of BF_2dbmPLA, this impressive optical phenomenon is still readily observable for PCL-PLA materials, even with the naked eye (Tables 4 and 5 and Figure 6). Additionally, the RTP emission is dependent on both the PLA chain length and the stereochemistry. When the PLA segment is longer, the emission is slightly blue-shifted and more narrow, and RTP intensity increases. Visually, the D,L-polymer emission is brighter than the L-material at comparable molecular weights.

Observations regarding emission intensities correlate well with lifetime measurements. Both fluorescence and RTP lifetimes can be fit to triple exponential decays, which is common given the heterogeneous environments in the polymer films.[6] Better fits are obtained for polymers with higher MWs given that the fluorophores may be more evenly distributed, similar to solution properties. The fluorescence lifetime, τ_F, of BF_2dbmPCL (powder: 15.6 ns; film: 2.64 ns) is longer than that for the block copolymers (powders: 3.54−4.07 ns; films: 2.18−2.61 ns). Although the values are very close for the diblocks, slightly longer lifetimes are measured for shorter chain lengths. The RTP lifetime, τ_{RTP}, in contrast, is the longest for the BF_2dbmPCL-PLA polymer with the highest MW (18.6 kDa, powder: 266 ms; film: 154 ms). Furthermore, the powder samples all exhibit much longer RTP lifetimes than those of films. Slight inconsistency in RTP lifetimes is noticed for low MW polymers when they are in different forms. For films, the lifetime is reduced almost eight-fold for BF_2dbmPCL-PLLA with the lowest MW (11.2 kDa, 22 ms). However, short-chain BF_2dbmPCL-PLA has the shortest τ_{RTP} among powder samples (92.4 ms). Again, these differences between powder and film samples could be caused by polymer processing, substrate effects, or enhanced susceptibility of film samples to trace

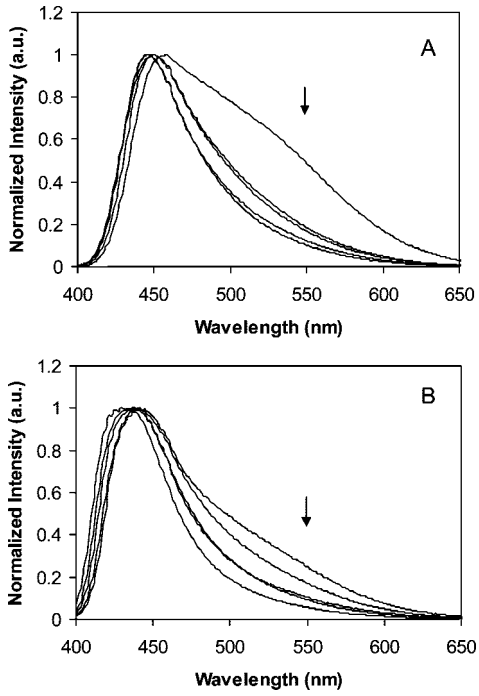

Figure 5. Fluorescence emission spectra for (A) powders and (B) spin-cast films of BF_2dbmPCL, BF_2dbmPCL-PLLA (11 100 Da), BF_2dbmPCL-PLA (11 200 Da), BF_2dbmPCL-PLLA (15 000 Da), and BF_2dbmPCL-PLA (18 600 Da) (order indicated by the arrows).

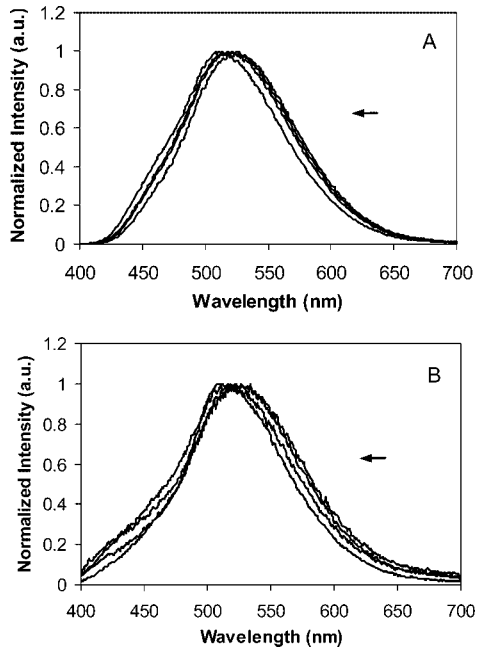

Figure 6. RTP emission spectra for (A) powders and (B) spin-cast films of BF_2dbmPCL-PLLA (11 100 Da), BF_2dbmPCL-PLA (11 200 Da), BF_2dbmPCL-PLLA (15 000 Da), and BF_2dbmPCL-PLA (18 600 Da) (order indicated by the arrows). (Note: No RTP for BF_2dbmPCL.)

quenchers. Further investigations of polymer processing effects are merited.

As in previous studies with PLA[6,7,17] and PCL[25] homopolymers as well as here with blocks, polymer composition affects the emissive properties of boron dye−polymer conjugates. One possible model for explaining these observations relies on differences in polymer free volume (V_f)[37] in these polyester materials. Polymer local V_f is a parameter that is used to describe the microcavities in condensed polymer media.[38] Loutfy[39] has reported that certain nonaromatic, double-bond-containing, fluorescent, malonitrile dye derivatives can be used to probe V_f on the basis of the sensitivity of their fluorescence to different polymer compositions or molecular weights. These "rotamer dyes" are donor−acceptor organic molecules with dramatic conformational relaxation, which decay nonradiatively in free media such as organic solvents. However, when the dyes are placed in polymer matrices, small V_f may restrict rotations and thus increase the fluorescence quantum yield of the dye. For example, a sudden increase in intensity was observed for the dye probe in an ongoing polymerization of styrene when the molecular weight of the polymer exceeded 10 kDa. The change in intensity was correlated to the morphological change of polystyrene beyond 10 kDa, hypothesized to relate to the critical entanglement length, which corresponds to a V_f decrease.[40]

Along with the molecular weight effect, Loutfy[41] also found that other polymer composition effects, even differences in tacticity for the same polymer, could also influence the quantum yields of the dye probes. Later, Hill et al.[42] used a free volume approach to understand the mechanical behavior of miscible polycarbonate blends and pointed out that the degree of crystallinity in the polymeric system can influence V_f. Recently, De Shryver et al.[43] designed a real-time single molecule fluorescent probe that has a calculated van der Waals volume difference of 0.201 nm^3 between its two comformer states. When embedded in poly(methyl methacrylate) (mean $V_f = 0.105$ nm^3), the dye shows a lifetime distribution corresponding to single exponential decay (e.g., one emitting species or conformation in a uniform environment). A bimodal lifetime distribution was observed when the dye was blended with poly(*n*-butyl methacrylate) of significantly higher mean V_f (0.135 nm^3), attributed to different conformations. This experiment suggests that although the two polymers are quite similar in chemical composition, subtle differences can result in a perceivable change in the probe response. It is also important to note that even solid-state polymeric matrices are not static but are dynamic environments where the microcavities move about in the media. Van Hulst et al.[44] have demonstrated the use of dye triplet lifetime to study polymer V_f dynamics, where fluctuations in lifetimes were observed as a function of time.

Poly(ε-caprolactone) homopolymers are known to be more crystalline than PCL-PLA (or PLLA) block copolymers.[26] In the case of polycarbonates, a higher degree of crystallinity increases the size but decreases the number of microcavities in the amorphous region of the polymer because of the constraining force exerted by the crystalline regions. If PCL behaves similarly, that is, if dye molecules at the chain terminals of BF_2dbmPCL materials are excluded from the crystalline PCL microdomains and reside within the amorphous regions with nanometer-sized holes that are bigger than or comparable to the volume needed for increased dye movements, then they would possess greater rotational freedom, enhancing nonradiative over radiative triplet (i.e., RTP) decay pathways (Figure 7). PLLA is also a crystalline polymer; however, the T_g of PLLA is above room temperature (~60 °C; compare with PCL: T_g = −60 °C).[23,45] It is well known that V_f significantly increases above T_g.[46] Therefore, at room temperature, the PCL amorphous region could be much more fluid-like than the PLLA amorphous region, where chains are still "frozen" below T_g. In purely amorphous, glassy D,L-PLA systems, in contrast, the dye may be more evenly dispersed throughout the material, and the polymer may have lower free volume because the T_g of D,L-PLA is also above room temperature. The mechanism of long-lived and relatively strong RTP for solid-state BF_2dbmPLA may be related to restricted BF_2dbm motion and thus decreased thermal decay from the triplet excited state in the rigid solid matrix.[6] (RTP has previously been observed for dyes with restricted motion in rigid environments such as cyclodextrins,[47]

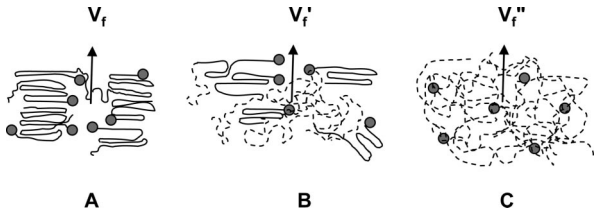

Figure 7. Model for polymer compositional effects on polymer free volume ($V_f > V_f' > V_f''$) (gray spheres: boron dyes; solid line: PCL; dashed line: PLA). (A) Semicrystalline BF_2dbmPCL, closer dye proximity, red-shifted fluorescence, greater freedom of motion, no RTP; (B) hybrid semicrystalline-amorphous BF_2dbmPCL-PLA, weak RTP; (C) amorphous BF_2dbmPLA, greater dye distances, blue-shifted fluorescence, restricted dye motion, stronger RTP.

glucose glass,[48] proteins,[49] or micelles.[50]) However, for BF_2dbmPCL-PLA block copolymers, PLA segments may disrupt the crystalline regions as well as increase the overall volume of amorphous regions. It is known that small segments of PLA can decrease PCL crystallinity dramatically.[23,26] Therefore, PLA blocks may decrease the size of the microcavities, limit the rotations and vibrations of the excited state dyes residing there, and decrease the probability of nonradiative, thermal decay pathways. As a result, the radiative triplet decay pathway is favored, and RTP is "turned on." According to this model and consistent with experimental observations, the strongest RTP is expected for entirely amorphous BF_2dbmPLA.

Both emission spectra and lifetime values are also in accord with the free volume hypothesis. When the size of the microcavities between crystalline domains is largest, dyes not only possess more rotational and vibrational degrees of freedom (and no RTP) if excluded from crystalline domains, but also are predicted to be in closer proximity to each other around the same cavity. The "forced contacts" and increased concentration of the BF_2dbm dye molecules around the large microcavities can correlate with greater fluorophore−fluorophore (F−F) interactions in the excited state and thus, increased singlet excited-state energy stabilization.[7] This is reflected in a red shift and broadening in the emission spectrum for BF_2dbmPCL versus block copolymer and BF_2dbmPLA materials (Figure 5). Furthermore, this interaction also decreases the singlet−triplet energy splitting and facilitates thermal back population from the long-lived triplet state to the singlet excited state. The RTP lifetimes can be significantly reduced because of this back population pathway and delayed fluorescence. This argument can help to explain the polymer chain length and isomer dependence. Longer chain length results in reduced F−F interaction and higher emitting energy, so the spectrum is blue-shifted. As explained above, a higher degree of crystallinity increases F−F interactions, resulting in a red-shifted spectrum for semicrystalline PLLA versus amorphous PLA. Clearly, the luminescence data and trends observed in this study are inconsistent with a simplistic understanding of RTP probability increasing with increasing matrix rigidity. A different explanation is required.

Conclusions

In summary, BF_2dbmPCL-PLA block copolymers were synthesized from a boron PCL macroinitiator. Both PLA and PLLA analogues were prepared for comparison. Thermal properties, namely, decomposition, glass transition, and melting temperatures, are typical for these polyester materials. All materials exhibit nearly identical intense blue fluorescence in solution, however optical properties are different in the solid state. Although room temperature phosphorescence is noted for BF_2dbmPLA homopolymers, it is absent for BF_2dbmPCL materials.[25] Normally, RTP is enhanced in rigid matrices because of restricted degrees of freedom and thus fewer thermal decay pathways for the dye.[47−50] For boron dyes in PCL, data suggest that the dye chain ends may be functioning as impurities that are excluded from polymer crystalline regions; instead, they may be concentrated in the amorphous regions between crystalline domains, where there are microcavities, greater free volume, and thus more degrees of freedom for the dye. When PLA or PLLA segments are grown from BF_2dbmPCL macroinitiators, however, the RTP is restored for the resulting block copolymer products. Both RTP intensities and lifetimes increase with longer PLA or PLLA segments, and stronger RTP is observed for the less crystalline PCL-PLA copolymer. These findings point to the utility of difluoroboron diketonate dyes as probes of polymer properties and microdomains. Their fluorescence is sensitive to the polarity of the surrounding medium, both solvent and polymer composition as well as dye−dye interactions (i.e., dye concentration or polymer MW effects). Dye phosphorescence, however, is sensitive to the polymer microstructure. Investigation of other polymer compositions is underway to explore these possibilities further. This family of stimuli-responsive boron biomaterials is also being utilized as imaging agents and oxygen sensors in cells, tissues, and in vivo.

Acknowledgment. We thank the National Science Foundation (CHE 0718879) for support for this research.

References and Notes

(1) (a) Nagai, A.; Miyake, J.; Kokado, K.; Nagata, Y.; Chujo, Y. *J. Am. Chem. Soc.* **2008**, *130*, 15276–15278. (b) Nagai, A.; Kodado, K.; Nagata, Y.; Chujo, Y. *Macromolecules* **2008**, *41*, 8295–8298. (c) Nagata, Y.; Chujo, Y. *Macromolecules* **2008**, *41*, 2809–2813. (d) Nagata, Y.; Otaka, H.; Chujo, Y. *Macromolecules* **2008**, *41*, 737–740.
(2) Zhu, M.; Jiang, L.; Yuan, M.; Liu, X.; Ouyang, C.; Zheng, H.; Yin, X.; Zuo, Z.; Liu, H.; Li, Y. *J. Polym. Sci., Part A: Polym. Chem.* **2008**, *46*, 7401–7410.
(3) (a) Qin, Y.; Kiburu, I.; Shah, S.; Jäkle, F. *Macromolecules* **2006**, *39*, 9041–9048. (b) Parab, K.; Venkatasubbaiah, K.; Jäkle, F. *J. Am. Chem. Soc.* **2006**, *128*, 12879–12885. (c) Jäkle, F. *Coord. Chem. Rev.* **2006**, *250*, 1107–1121.
(4) Wang, Z.-Y.; Weck, M. *Macromolecules* **2005**, *38*, 7219–7224.
(5) (a) Cogné-Laage, E.; Allemand, J.-F.; Ruel, O.; Baudin, J.-B.; Croquette, V.; Blanchard-Desce, M.; Jullien, L. *Chem.—Eur. J.* **2004**, *10*, 1445–1455. (b) Chow, Y. L.; Johansson, C. I. *J. Phys. Chem.* **1995**, *99*, 17558–17565.
(6) Zhang, G.; Chen, J.; Payne, S. J.; Kooi, S. E.; Demas, J. N.; Fraser, C. L. *J. Am. Chem. Soc.* **2007**, *129*, 8942–8943.
(7) Zhang, G.; Kooi, S. E.; Demas, J. N.; Fraser, C. L. *Adv. Mater.* **2008**, *20*, 2099–2104.
(8) For a related concept, see: Bulovic, V.; Deshpande, R.; Thompson, M. E.; Forrest, S. R. *Chem. Phys. Lett.* **1999**, *308*, 317–322.
(9) Vo-Dinh, T. *Room Temperature Phosphorimetry for Chemical Analysis*; Wiley: New York, 1984.
(10) Niday, G. J.; Seybold, P. G. *Anal. Chem.* **1978**, *50*, 1577–1578.
(11) Demas, J. N.; DeGraff, B. A. In *Topics in Fluorescence Spectroscopy*; Lakowicz, J. R., Ed.; Plenum Press: New York, 1994; Vol. 4, pp 71−107.
(12) Saviotti, M. L.; Galley, W. C. *Proc. Natl. Acad. Sci. U.S.A.* **1974**, *71*, 4154–4158.
(13) Vanderkooi, J. M.; Englander, S. W.; Papp, S.; Wright, W. W.; Owen, C. S. *Proc. Natl. Acad. Sci. U.S.A.* **1990**, *87*, 5099–5103.
(14) Schlyer, B. D.; Steel, D. G.; Gafni, A. *J. Biol. Chem.* **1995**, *270*, 22890–22894.
(15) Aizawa, H.; Katsumata, T.; Takahashi, J.; Matsunaga, K.; Komuro, S.; Morikawa, T.; Toba, E. *Rev. Sci. Instrum.* **2003**, *74*, 1344–1349.
(16) Brinas, R. P.; Troxler, T.; Hochstrasser, R. M.; Vinogradov, S. A. *J. Am. Chem. Soc.* **2005**, *127*, 11851–11862.
(17) Pfister, A.; Zhang, G.; Zareno, J.; Horwitz, A. F.; Fraser, C. L. *ACS Nano* **2008**, *2*, 1252–1258.
(18) (a) Clark, J. H. *Green Chem.* **1999**, *1*, 1–8. (b) Anastas, P. T.; Kirchhoff, M. M. *Acc. Chem. Res.* **2002**, *35*, 686–694. (c) Thomas, J. M.; Raja, R. *Annu. Rev. Mater. Res.* **2005**, *35*, 315–350.
(19) Vink, E. T. H.; Rábago, K. R.; Glassner, D. A.; Springs, B.; O'Connor, R. P.; Kolstad, J.; Gruber, P. R. *Macromol. Biosci.* **2004**, *4*, 551–564.
(20) Auras, R.; Harte, B.; Selke, S. *Macromol. Biosci.* **2004**, *4*, 835–864.

(21) Griffith, L. G.; Naughton, G. *Science* **2002**, *295*, 1009–1014.
(22) Pitt, C. G.; Chasalow, F. I.; Hibionada, Y. M.; Klimas, D. M.; Schindler, A. *J. Appl. Polym. Sci.* **1981**, *26*, 3779–3787.
(23) Huang, S. J. In *Handbook of Biodegradable Polymers*; Bastioli, C., Ed.; Rapra Technology Limited: Shawbury, UK, 2005; pp 287−301.
(24) Sahoo, S. K.; Labhasetwar, V. *Drug Discovery Today* **2003**, *8*, 1112–1120.
(25) Zhang, G.; St. Clair, T. L.; Fraser, C. L. *Macromolecules*, in press.
(26) Cohn, D.; Salomon, A. H. *Biomaterials* **2005**, *26*, 2297–2305.
(27) Hu, Y.; Jiang, X.; Ding, Y.; Zhang, L.; Yang, C.; Zhang, J.; Chen, J.; Yang, Y. *Biomaterials* **2003**, *24*, 2395–2404.
(28) Reeve, M. S.; McCarthy, S. P.; Downey, M. J.; Gross, R. A. *Macromolecules* **1994**, *27*, 825–831.
(29) Ishii, D.; Ying, T. H.; Mahara, A.; Murakami, S.; Yamaoka, T.; Lee, W.-k.; Iwata, T. *Biomacromolecules* **2009**, *10*, 237–242.
(30) Demas, J. N.; Crosby, G. A. *J. Phys. Chem.* **1971**, *75*, 991–1024, section II.C.2, equation 16.
(31) Melhuish, W. H. *J. Phys. Chem.* **1961**, *65*, 229–235.
(32) Fiore, G. L.; Fraser, C. L. *Macromolecules* **2008**, *41*, 7892–7897.
(33) Huang, M.-H.; Li, S.; Coudane, J.; Vert, M. *Macromol. Chem. Phys.* **2003**, *204*, 1994–2001.
(34) Sivalingam, G.; Madras, G. *Polym. Degrad. Stab.* **2004**, *84*, 393–398.
(35) Lemmouchi, Y.; Perry, M. C.; Amass, A. J.; Chakraborty, K.; Schacht, E. *J. Polym. Sci., Part A: Polym. Chem.* **2008**, *46*, 5348–5362.
(36) Carraway, E. R.; Demas, J. N.; DeGraff, B. A.; Bacon, J. R. *Anal. Chem.* **1991**, *63*, 337–342.
(37) (a) Doolittle, A. K. *J. Appl. Polym. Sci.* **1951**, *22*, 1471–1475. (b) Williams, M. L.; Landel, R. F.; Ferry, J. D. *J. Am. Chem. Soc.* **1955**, *77*, 3701–3707.
(38) Victor, J. G.; Torkelson, J. M. *Macromolecules* **1987**, *20*, 2241–2250.
(39) Loutfy, R. O. *Pure Appl. Chem.* **1986**, *9*, 1239–1248.
(40) Loutfy, R. O. *Macromolecules* **1983**, *16*, 678–680.
(41) Loutfy, R. O. *Macromolecules* **1983**, *16*, 452–456.
(42) (a) Hill, A. J.; Zipper, M. D.; Tant, G. M.; Jordan, T. C.; Shultz, A. R. *J. Phys.: Condens. Matter* **1996**, *8*, 3811–3827. (b) Zipper, M. D.; Simon, G. P.; Cherry, P.; Hill, A. J. *J. Polym. Sci., Part B: Polym. Phys.* **1994**, *32*, 1237–1247.
(43) Vallée, R. A. L.; Cotlet, M.; Van Der Auweraer, M.; Hofkens, J.; Müllen, K.; De Schryver, F. C. *J. Am. Chem. Soc.* **2004**, *126*, 2296–2297.
(44) Veerman, J. A.; Garcia-Parajo, M. F.; Kuipers, L.; van Hulst, N. F. *Phys. Rev. Lett.* **1999**, *83*, 2155–2158.
(45) Pitt, C. G. In *Drugs and Pharmaceutical Sciences*; Chasin, M., Langer, R., Eds.; Marcel Dekker: New York, 1990; Vol. 45, pp 71−120.
(46) The Fox−Flory equation: $V_f = K + (\alpha_R - \alpha_G)T$, where K is the polymer free volume at 0 K, α_G is the cubic volume expansion coefficient when the polymer is in the glassy state, α_R is the cubic volume expansion coefficient when the polymer is in the rubbery state, and T is temperature.
(47) Li, S.; Purdy, W. C. *Chem. Rev.* **1992**, *92*, 1457–1470.
(48) Wang, J.; Hurtubise, R. *J. Anal. Chem.* **1997**, *69*, 1946–1951.
(49) Saviotti, M. L.; Galley, W. C. *Proc. Nat. Acad. Sci. U.S.A.* **1974**, *71*, 4154–4158.
(50) Love, L. J. C.; Skrilec, M.; Habarta, J. G. *Anal. Chem.* **1980**, *52*, 754–759.

MA9000622